scientific reports

Check for updates

OPEN

Expression analysis and possible functional roles of semaphorin/plexin/CRMP families in mouse pancreatic islets

Mayu Kyohara[1], Rie Takayanagi[1], Takahiro Tsuno[2], Esther Ong Yajima[2], Ryota Inoue[2], Naoya Yamashita[4], Tomoko Okuyama[1], Kuniyuki Nishiyama[2,3], Kohichi Matsunaga[2], Emi Ishida[2], Shuichi Ito[3], Yasuo Terauchi[1], Yoshio Goshima[4] & Jun Shirakawa[1,2]✉

Semaphorins were initially identified as axon guidance molecules that were widely expressed and involved in divergent functions in various organs, including neuronal development and immunological processes. Collapsin response mediator proteins (CRMPs) are involved in the intracellular signaling of semaphorin 3A (Sema3a) and are highly expressed in the nervous system. However, the participation of semaphorins or their receptors plexins and CRMPs in the regulation of islet function remains unknown. In this study, we measured the expression of semaphorin, plexin, and CRMP families in mouse islets, and their expression levels were altered by treatment with high glucose or a glucokinase activator (GKA). The expression and phosphorylation of CRMP-2 in islets were upregulated in high-fat diet (HF)-fed obese mice, and the expression of CRMP-2 was downregulated in islets from *db/db* mice. HF-fed *CRMP-2* knockout mice exhibited impaired glucose tolerance. These results indicated that the semaphorin/plexin/CRMP families in mouse islets might be involved in glucose metabolism partly through glucose/glucokinase.

Keywords Semaphorin, Plexin, CRMP-2, Glucokinase, Glucokinase activator, Diabetes

Glucose/glucokinase-induced glycolysis triggers insulin secretion and regulates β-cell proliferation and survival in pancreatic islets[1]. Previous studies have shown that ER stress-related molecules, cell cycle regulators, inflammatory proteins, and extracellular matrix proteins are involved in the glucokinase-mediated glucose signaling pathway in β-cells[2,3], but the precise molecular mechanism involved remains unclear.

Semaphorins, which were initially identified as axon guidance molecules, include more than 20 members grouped into eight classes and are highly expressed in the developing and adult nervous system. Semaphorins are involved not only in neuronal development[4,5] but also in the functions of various tissues, including the immune system[6], cardiovascular development[7], bone metabolism[8], and cancer progression[9]. In the context of diet-induced obesity, the signaling of semaphorin 3E (Sema3e) and its receptor plexin-D1 reportedly induces inflammation in adipose tissue via the infiltration of macrophages, which leads to systemic insulin resistance[10]. In addition, excess secretion of semaphorin 3A (Sema3a) from podocytes promotes severe diabetic nephropathy by disrupting the glomerular filtration barrier[11]. Although plexins, receptors of semaphorins, are generally required for the development of the nervous system through semaphorins[12–14], the participation of semaphorins and plexins in the function of pancreatic islet cells is unknown. CRMPs are involved in the intracellular signaling of Sema3a and are highly expressed in the developing and adult nervous system[15,16]. The CRMP family has multiple functions in neuronal development, including axon formation and extension, axon guidance, and neuronal polarity[17,18]. Although CRMP-2 is phosphorylated by Gsk-3β, which works to regulate insulin signaling[19–21], there have been no reports that CRMPs play roles in glucose metabolism. Furthermore, several semaphorins, termed "immune semaphorins", are well established as key regulators of immune responses. Given that type 1 diabetes is an autoimmune disease, it is plausible that semaphorins, along with their receptor plexins, and CRMPs, contribute to its onset or pathogenesis.

[1]Department of Endocrinology and Metabolism, Graduate School of Medicine, Yokohama City University, Yokohama, Japan. [2]Laboratory of Diabetes and Metabolic Disorders, Institute for Molecular and Cellular Regulation (IMCR), Gunma University, Maebashi, Japan. [3]Department of Pediatrics, Graduate School of Medicine, Yokohama City University, Yokohama, Japan. [4]Department of Molecular Pharmacology and Neurobiology, Graduate School of Medicine, Yokohama City University, Yokohama, Japan. ✉email: jshira@gunma-u.ac.jp

We previously performed gene expression analysis in islets after treatment with a glucokinase activator (GKA)[22] and revealed that the expression of several genes related to the central nervous system, including semaphorins, was altered by glucokinase activation. In this study, we analyzed the expression of semaphorins, plexins, and CRMPs in mouse islets and explored the possible roles of these molecules in glucose metabolism.

Results

Sema3c/Sema5a expression in mouse islets is controlled by glucose signaling

We previously performed global gene expression analysis in mouse islets in the presence or absence of a glucokinase activator (GKA) for 24 h[22]. Gene Ontology analysis of genes significantly upregulated (> 2-fold) or downregulated (< 0.5-fold) by GKA (*$P < 0.05$) suggested a possible involvement in the nervous system, such as "neuron projection" (ex. synaptotagmin 5 (*Syt5*), neuromedin B (*Nmb*)), and "chemical synaptic transmission" (ex. 5-hydroxytryptamine receptor 6 (*Htr6*), glutamate receptor, metabotropic 2 (*Grm2*), and "central nervous system projection neuron axonogenesis" (ex. nuclear receptor subfamily 4, group A, member 2 (*Nr4a2*), doublecortin (*Dcx*)) (Fig. 1a). In the cluster analysis, the term "central nervous system projection neuron axonogenesis" was grouped into the same cluster as "neuron migration" (ex. astrotactin 1 (*Astn1*), doublecortin-like kinase 1 (*Dclk1*)), "nervous system development" (ex. SH3/ankyrin domain gene 1 (*Shank1*), neurotrophic tyrosine kinase, receptor, type 2 (*Ntrk2*)), and "axon guidance" (ex. semaphorin 3c (*Sema3c*), and semaphorin 5a (*Sema5a*)) (Fig. 1a). Furthermore, we conducted a canonical pathway analysis of the genes differentially expressed by GKA (*$P < 0.05$) using Ingenuity Pathway Analysis (IPA) and identified several significantly enriched pathways, including "axonal guidance signaling" (ex. *Sema3c*, *Sema5a*) (Fig. 1b). We noted that the expression of two semaphorins was altered; the expression of *Sema3c* was upregulated (10.8-fold, $P < 0.01$) and that of *Sema5a* was downregulated (0.2-fold, $P < 0.01$) by GKA in mouse islets. An increase in *Sema3c* and a decrease in *Sema5a* expression were detected in GKA-treated islets, and these effects occurred in a time- and glucose concentration-dependent manner (Fig. 2a-b).

Next, we analyzed the mRNA expression levels of *Sema3c* and *Sema5a* in the islets of diabetic mice. The upregulation of *Sema3c* by GKA was suppressed, but the downregulation of *Sema5a* by GKA was preserved in the islets of insulin receptor substrate (*IRS*)-2 knockout mice, which exhibit reduced β-cell proliferation and systemic insulin resistance[23] (Fig. 2c). The *db/db* mice, a model of morbid obesity and severe hyperglycemia with insulin resistance[24], exhibited impaired *Sema3c* upregulation but not *Sema5a* downregulation after stimulation with GKA (Fig. 2d). In the islets of high-fat diet (HF)-fed obese mice, the upregulation of *Sema3c* expression by GKA was augmented more than that in normal chow (NC)-fed mice, similar to the increase in *IRS-2* expression (Fig. 2e). These results indicated that *Sema3c* upregulation is mediated by insulin signaling pathways including the IRS-2.

We further analyzed the regulatory mechanisms underlying *Sema3c* expression in mouse islets. *Sema3c* upregulation by GKA was inhibited by MH (D-mannoheptulose), a glucokinase inhibitor (Fig. 2f), whereas diazoxide (K^+ ATP channel opener) did not (Fig. 2g). Because glucose-induced IRS-2 expression in β-cells is thought to be mediated by Ca^{2+}-dependent calcineurin signaling[25], we evaluated the expression levels of *IRS-2* and *Sema3c* in islets treated with nifedipine, a calcium channel blocker, or FK506, a calcineurin inhibitor. While *IRS-2* upregulation by GKA was blunted by both nifedipine and FK506, FK506 did not affect *Sema3c* upregulation by GKA (Fig. 2h). *Sema3c* expression was amplified by treatment with thapsigargin, an inhibitor of sarcoplasmic/endoplasmic reticulum (ER) Ca^{2+} ATPases, at various glucose concentrations (Fig. 2i), whereas GKA did not cause further amplification of *Sema3c* expression in the presence or absence of diazoxide (Fig. 2j).

Detection of *Sema3c* and *Sema5a* expression in islet β and non-β cells by single-cell RNA sequencing

We conducted a reanalysis of previously published single-cell RNA sequencing datasets of pancreatic islets from normal chow-fed and 8-week high-fat diet (HF)-fed mice to investigate the expression of *Sema3c* and *Sema5a* in β-cells and non-β islet cells[26]. Either *Sema3c*- or *Sema5a*-positive cells were identified not only in β-cells but also in α-cells and other non-β endocrine cells within the islets (Supplementary Fig. 1a-d). Notably, HF feeding led to an upregulation of *Sema3c* and *Sema5a* expression predominantly in β-cells. Pathway analysis of differentially expressed genes in *Sema3c*-positive β-cells from HF-fed mice showed enrichment in pathways associated with proteolysis and apoptosis (Supplementary Fig. 1e-f).

The expression of semaphorins, plexins, and CRMPs in metabolic tissues

We next investigated the expression of other semaphorins in metabolic organs, including the brain, liver, adipose tissue, skeletal muscle, and islets, from C57BL/6J mice by using quantitative real-time PCR (Fig. 3a-c).

Some semaphorins, plexins, and CRMPs were predominantly expressed in brain tissues (Fig. 3a-c). The expression levels of *Sema4f*, *Sema7a*, *Plexin-A4*, *Plexin-C1*, and *CRMP-2* were highest in the cerebral cortex, and those of *Sema3a*, *Sema3d*, *Sema3e*, *Sema5a*, *Sema5b*, *Sema6a*, *Sema6b*, *Plexin-A3*, *Plexin-B1*, *Plexin-B3*, *CRMP-1*, *CRMP-3*, *CRMP-4*, and *CRMP-5* were highest in the olfactory bulb. *Sema4a* and *Sema4g* had the highest expression in the liver. Sema4A plays a role in the immune system and inflammatory diseases, especially multiple sclerosis[27]. *Sema3e* and *Plexin-D1* are expressed at low levels in adipose tissue, as they reportedly induce the infiltration of macrophages into adipose tissue[10]. *Sema3b*, *Sema3c*, *Sema3g*, *Sema4c*, *Sema4d*, *Sema6c*, *Plexin-A1*, and *Plexin-D1* were predominantly expressed in skeletal muscle. We also detected abundant *Sema3f*, *Sema4b*, *Sema6d*, *Plexin-A2*, and *Plexin-B2* expression in islets. There have been no previous reports that semaphorins and plexins are involved in the regulation of islet cell functions, such as insulin secretion and β-cell proliferation. *Sema3c* and *Sema5a*, whose expression levels in islets are regulated by glucose/GKA stimulation, as mentioned above, were detected at even lower levels in islets than in other tissues.

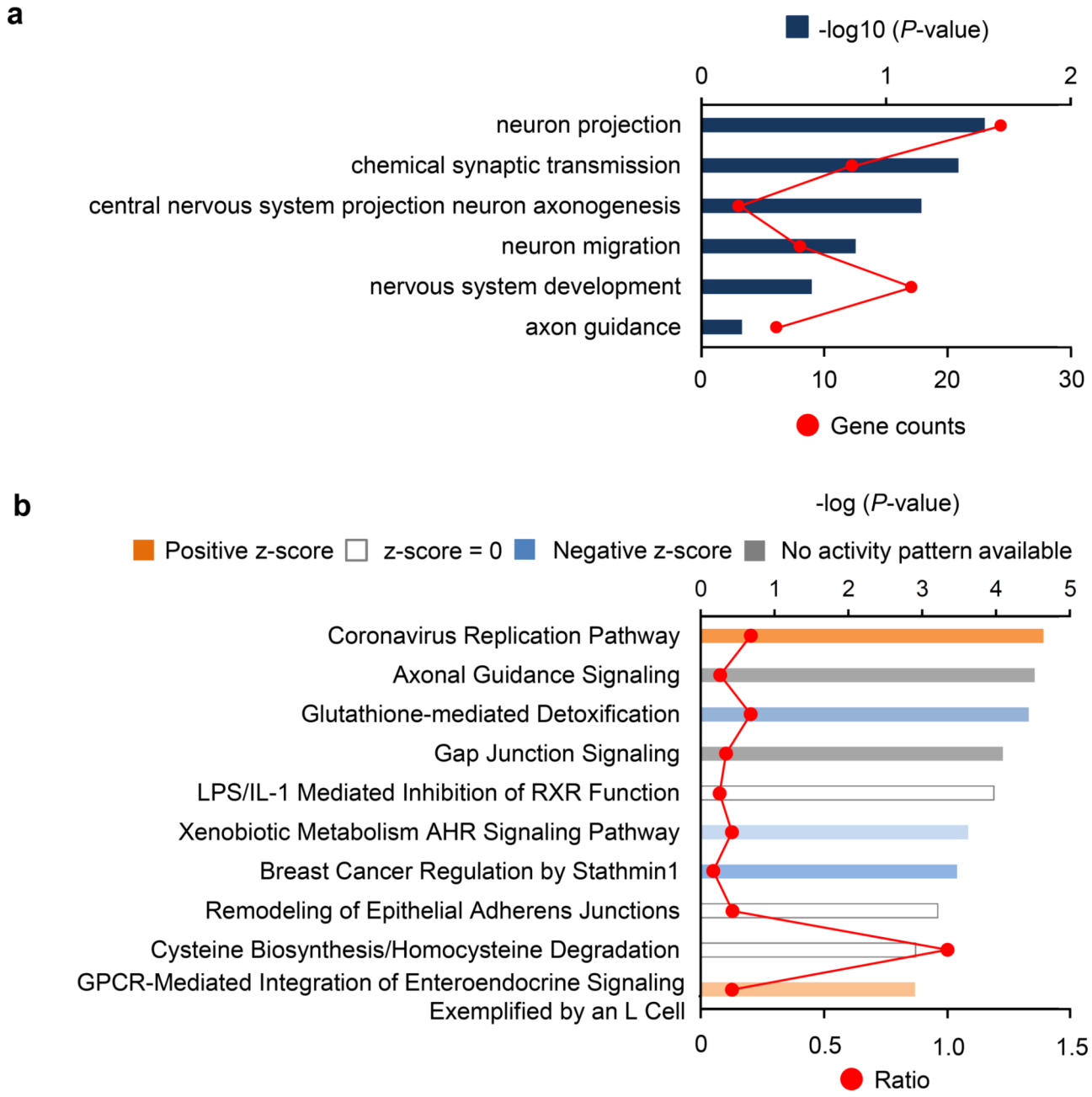

Fig. 1. Genes differentially expressed by GKA were suggested to be involved in the nervous system. **a**: Gene Ontology (GO) analysis of the genes that were significantly upregulated (>2-fold, $P<0.05$) or downregulated (<0.5-fold, $P<0.05$) by GKA was performed by using DAVID (https://david.ncifcrf.gov/). GO annotations related to the nervous system are shown here. The red line and markers show the number of genes differentially expressed by GKA for each GO annotation. **b**: The top 10 canonical pathway analyses of the genes that were significantly upregulated ($P<0.05$) or downregulated ($P<0.05$) by GKA were performed by using Ingenuity Pathway Analysis (IPA; www.ingenuity.com). The orange bar represents a positive z score that indicates that the pathway is activated. The blue bar represents a negative z score that indicates that the pathway is inhibited. The white bar represents a zero z score. The gray bar indicates that the activity pattern was not detected by IPA. The red line and markers show the ratio of the number of genes differentially expressed by GKA found in each pathway to the total number of genes in that pathway from within the IPA knowledge base.

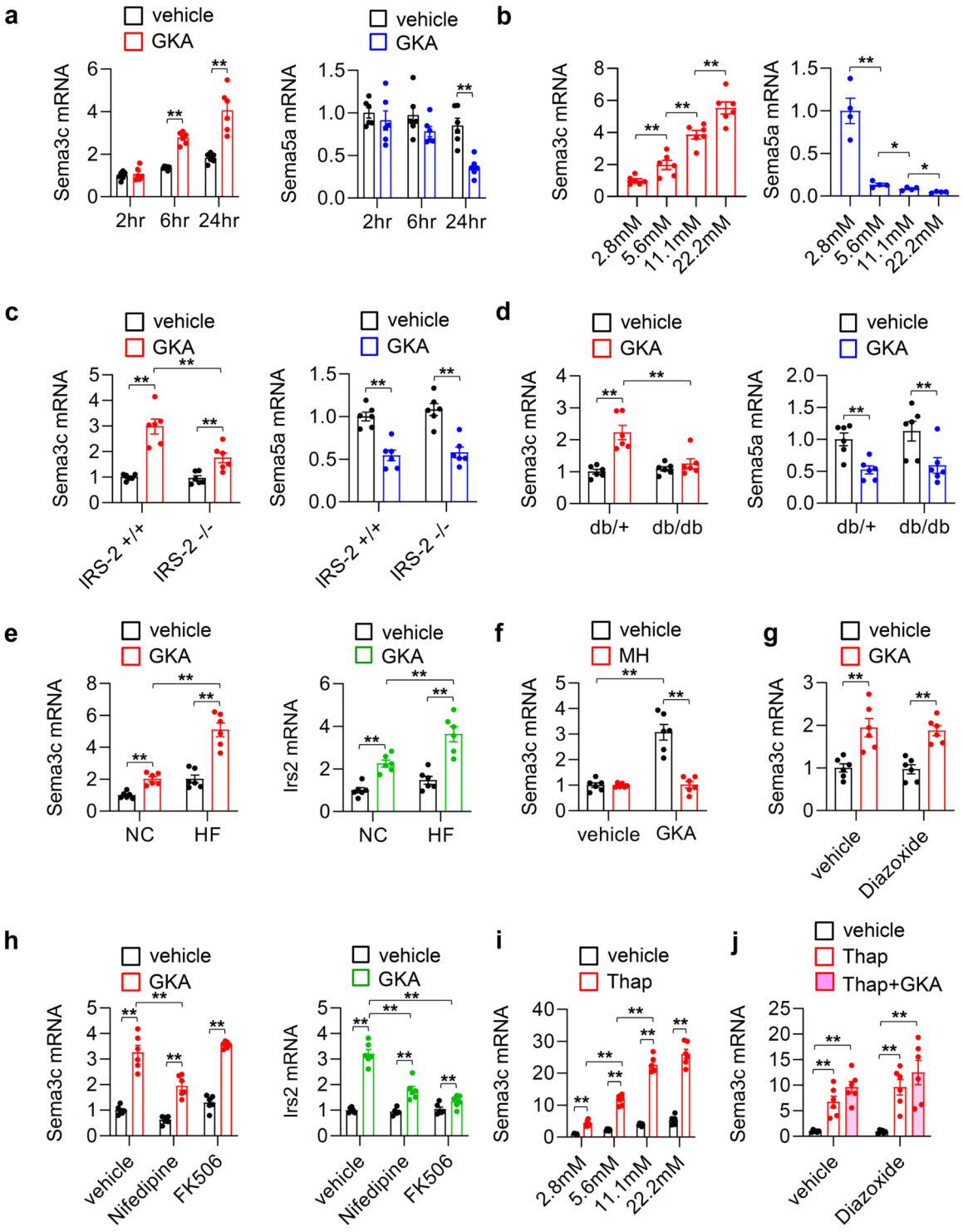

The impact of glucose metabolism on the expression of semaphorins, plexins, and CRMPs in mouse islets

Next, we determined the expression levels of semaphorins, plexins, and CRMPs in mouse islets treated with glucose or GKA or in islets from *db/db* mice (Fig. 4a-c). Figure 4a shows the expression levels of genes in islets from wild-type mice incubated with media supplemented with low (3.9 mmol/L) or high (16.7 mmol/L) glucose for 24 h. Consistent with the findings in Fig. 2b, *Sema3c* expression exhibited tendency toward upregulation in islets under high-glucose conditions. In contrast, the expression of *Sema5a*, *Plexin-A1*, and *Plexin-A3* was significantly downregulated in islets under high glucose conditions ($P < 0.05$, Fig. 4a). Figure 4b indicated the gene expression in islets treated with GKA or vehicle for 24 h. GKA induced significant changes in the expression of genes that were downregulated by *Plexin-D1* ($P < 0.05$, Fig. 4b). The increase in *Sema3c* and decrease in *Sema5a* expression levels by high glucose or GKA stimulation did not reach statistical significance in these experiments.

◀**Fig. 2**. *Sema3c*/*Sema5a* expression in mouse islets is controlled by glucose signaling. **a**: The mRNA expression levels of *Sema3c* and *Sema5a* at the indicated times in islets isolated from 8- to 10-week-old C57BL/6J mice incubated with GKA or vehicle (DMSO) for 24 h ($n = 6$; ANOVA). **b**: *Sema3c* and *Sema5a* expression levels in islets isolated from 8–10-week-old C57BL/6J mice incubated in the presence of 2.8, 5.6, 11.1, or 22.2 mmol/L glucose ($n = 4$–6; ANOVA). **c**: The mRNA expression levels of *Sema3c* and *Sema5a* in islets isolated from 12-week-old *IRS-2*$^{-/-}$ and *IRS-2*$^{+/+}$ mice incubated with GKA or vehicle (DMSO) for 24 h ($n = 6$; ANOVA). **d**: The mRNA expression levels of *Sema3c* and *Sema5a* in the islets of 8-week-old *db/db* and *db/+* mice incubated with GKA or vehicle (DMSO) for 24 h ($n = 6$; ANOVA). **e**: The mRNA expression levels of *Sema3c* and *IRS-2* in islets isolated from 12-week-old normal chow (NC)-fed mice and 20-week-old high-fat diet (HF)-fed mice incubated with GKA or vehicle (DMSO) for 24 h ($n = 6$; ANOVA). **f**: *Sema3c* expression in islets isolated from 8- to 10-week-old C57BL/6J mice incubated with GKA or vehicle (DMSO) with/without D-mannoheptulose (MH) ($n = 6$; ANOVA). **g**: *Sema3c* expression levels in islets isolated from 8–10-week-old C57BL/6J mice incubated with GKA or vehicle (DMSO) with/without diazoxide ($n = 6$; ANOVA). **h**: The mRNA expression levels of *Sema3c* and *IRS-2* in islets isolated from 8- to 10-week-old C57BL/6J mice incubated with GKA or vehicle (DMSO) with/without nifedipine or FK506 ($n = 6$; ANOVA). **i**: *Sema3c* expression levels in islets isolated from 8–10-week-old C57BL/6J mice incubated with thapsigargin (Thap) or vehicle (DMSO) in the presence of 2.8, 5.6, 11.1, or 22.2 mmol/L glucose ($n = 6$; ANOVA). **j**: *Sema3c* expression levels in the islets of 8- to 10-week-old C57BL/6J mice incubated with thapsigargin (Thap) and GKA in the presence of diazoxide or vehicle (DMSO) ($n = 6$; ANOVA). Islets were incubated in the presence of 5.6 mmol/L glucose (**a**, **c**-**h**, and **j**). The relative values were presented with C57BL/6J mouse islets treated with vehicle after 2 h incubation (**a**), C57BL/6J mouse islets under 2.8mM glucose (**b** and **i**), *IRS-2*$^{+/+}$ mouse islets treated with vehicle (**c**), *db/+* mouse islets treated with vehicle (**d**), NC-fed mouse islets treated with vehicle (**e**), and C57BL/6J mouse islets treated with vehicle (**f**-**h** and **j**) as the controls. The results are expressed as the mean ± SE. $^{*}P < 0.05$, $^{**}P < 0.01$.

Glucose signaling promotes glucokinase activation; however, our results revealed that the expression levels of semaphorins, plexins, and CRMPs in islets were somewhat different under high glucose conditions (Fig. 4a) or GKA stimulation (Fig. 4b) for each molecule. Furthermore, we investigated the expression levels of genes in islets from 15-week-old *db/db* mice, which exhibited marked hyperglycemia and insulin resistance. In *db/db* islets, *Sema3a*, *Sema3c*, *Sema5a*, *Sema6a*, *Sema7a*, and *CRMP-4* expression was increased, and *Sema4d*, *CRMP-2*, and *CRMP-5* expression was significantly decreased ($P < 0.05$, Fig. 4c). *Sema3c* and *Sema5a* expression in islets did not differ between the 8-week-old *db/+* vehicle group and the *db/db* vehicle group, as shown in Fig. 2d, whereas in islets from 15-week-old *db/db* mice in Fig. 4c, *Sema3c* and *Sema5a* expression levels were greater in the *db/db* group than in the *db/+* group. This mismatch in the *Sema3c* and *Sema5a* expression levels between 8-week-old *db/db* mice might be due to β-cell dysfunction because *db/db* mice markedly develop obesity and hyperglycemia with age (the average body weights were 24.9 g and 40.6 g in 8-week-old *db/+* and *db/db* mice and 30.9 g and 55.5 g in 15-week-old *db/+* and *db/db* mice, respectively; the average blood glucose levels were 137.0 mg/dL and 471.8 mg/dL in 8-week-old *db/+* and *db/db* mice and 143.4 mg/dL and 533.0 mg/dL in 15-week-old *db/+* and *db/db* mice, respectively).

These results suggested that the expression levels of several semaphorins, plexins, and CRMPs were modified in mouse islets under glucose/GKA stimulation or in *db/db* islets, which might be involved in the pathogenesis of islet cells in diabetes.

Expression of CRMP-2 in the endocrine pancreas

CRMP-2 was identified as a molecule involved in the intracellular signaling of Sema3a, a member of the semaphorin family[15,16]. The expression level of *CRMP-2* decreased in *db/db* islets (Fig. 4c). Therefore, we focused on CRMP-2 in terms of glucose metabolism and islet function.

To analyze whether the CRMP-2 protein is expressed in pancreatic β-cells, we conducted immunostaining of pancreatic sections from C57BL/6J mice. CRMP-2 was expressed in both α- and β-cells (Fig. 5a). Additionally, we detected the expression of both CRMP-2 and its phosphorylation form, phospho-CRMP-2 (p-CRMP-2) in the pancreatic β-cell line MIN6 (Fig. 5b). Notably, CRMP-2 and p-CRMP-2 exhibited higher expression in the islets of HF-fed mice than in those of NC-fed mice (Fig. 5c). Furthermore, to elucidate the transcriptional regulation of CRMP-2 in metabolic disorders, we quantified its mRNA expression in islets isolated from obese and/or diabetic mice, including *db/db* mice and *IRS-2* knockout mice, by using quantitative real-time PCR. In islets isolated from *db/db* mice, *CRMP-2* expression was decreased compared to that in islets isolated from control *db/+* mice (Fig. 5d). On the other hand, *CRMP-1* expression did not differ between the 2 groups (Fig. 5d), consistent with the results shown in Fig. 4c. *CRMP-1* and *CRMP-2* expression did not differ between *IRS-2* knockout and wild-type mice (Fig. 5e). These results indicated that CRMP-2 expression in mouse islets could be regulated by glucose metabolism but also by the insulin signaling pathway.

CRMP-2 knockout mice showed glucose intolerance

To assess the involvement of CRMP-2 in glucose metabolism in vivo, we analyzed mice deficient in CRMP under normal chow (NC) or high-fat diet (HF) conditions. CRMP-1 can form heterotetramers with CRMP-2 under physiological conditions[28]; hence, we also analyzed *CRMP-1* knockout mice (*CRMP-1*$^{-/-}$) and *CRMP-2* knockout mice (*CRMP-2*$^{-/-}$). We also attempted to generate *CRMP-1*/*CRMP-2* double knockout mice; however, we were unable to obtain *CRMP-1*$^{-/-}$*CRMP-2*$^{-/-}$ mice, suggesting that this genotype may be embryonically lethal.

Neither the *CRMP-1*$^{-/-}$ nor the *CRMP-2*$^{-/-}$ mice showed significant changes in body weight gain, tissue weight, or insulin sensitivity before or after HF feeding (Supplementary Fig. 2a-f, Supplementary Table 1).

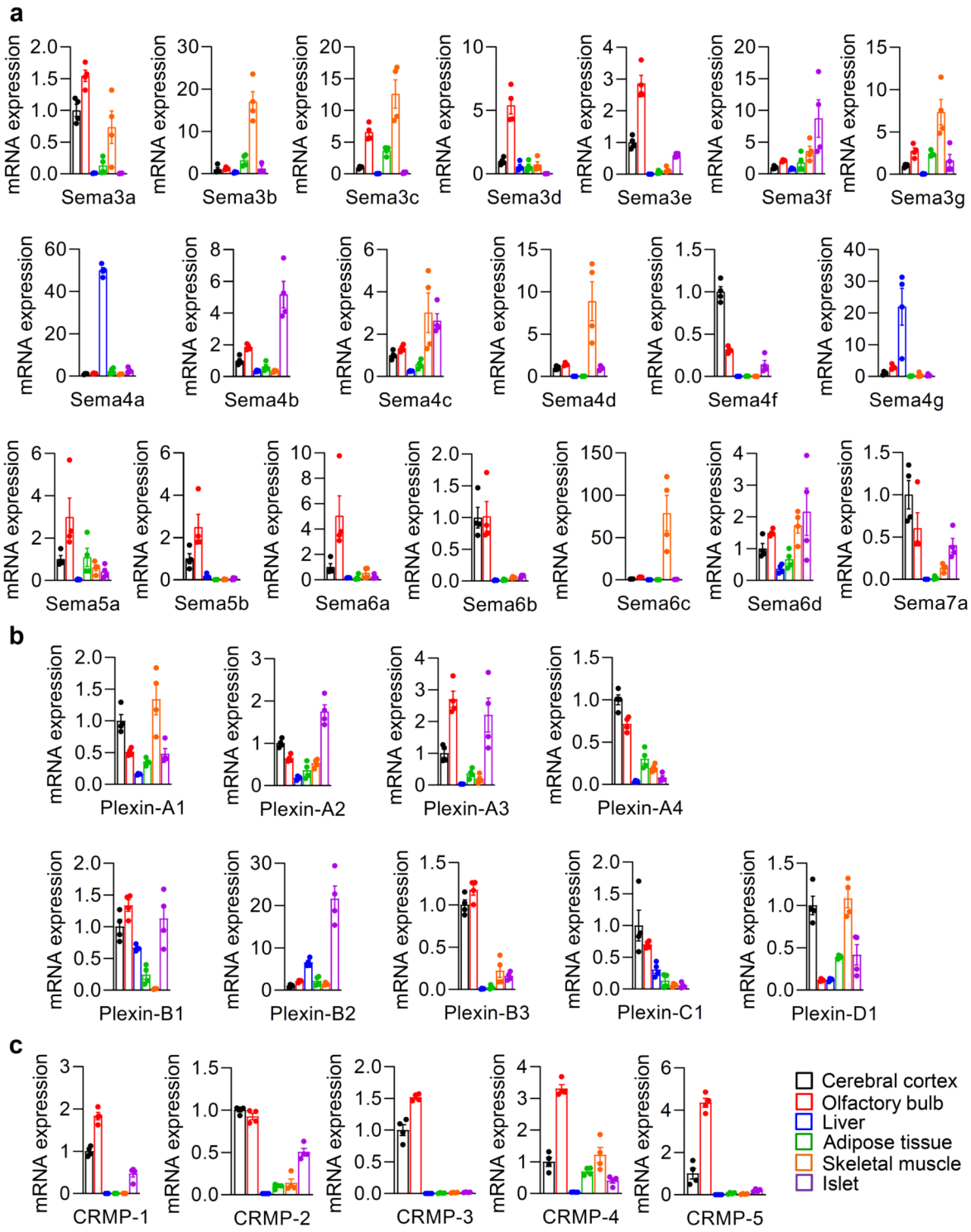

Fig. 3. Tissue semaphorin, plexin, and CRMP levels in metabolic organs from C57BL/6J mice. **a-c**: Semaphorin (**a**), plexin (**b**), and CRMP (**c**) mRNA expression levels in the cerebral cortex, olfactory bulb, liver, adipose tissue, skeletal muscle, and islets of 8- to 10-week-old C57BL/6J mice ($n = 4$ per group). The relative values were presented with cerebral cortex as the control.

CRMP-1$^{-/-}$ mice presented slight elevations in blood glucose levels during the GTT, which were omitted by the HF-induced metabolic load (Fig. 6a and c). There were no differences in insulin levels between *CRMP-1*$^{-/-}$ mice and wild-type controls under either NC- or HF-fed conditions (Fig. 6b and d). *CRMP-2*$^{-/-}$ mice exhibited slight glucose intolerance after HF feeding but not after NC feeding, even though there were no significant changes

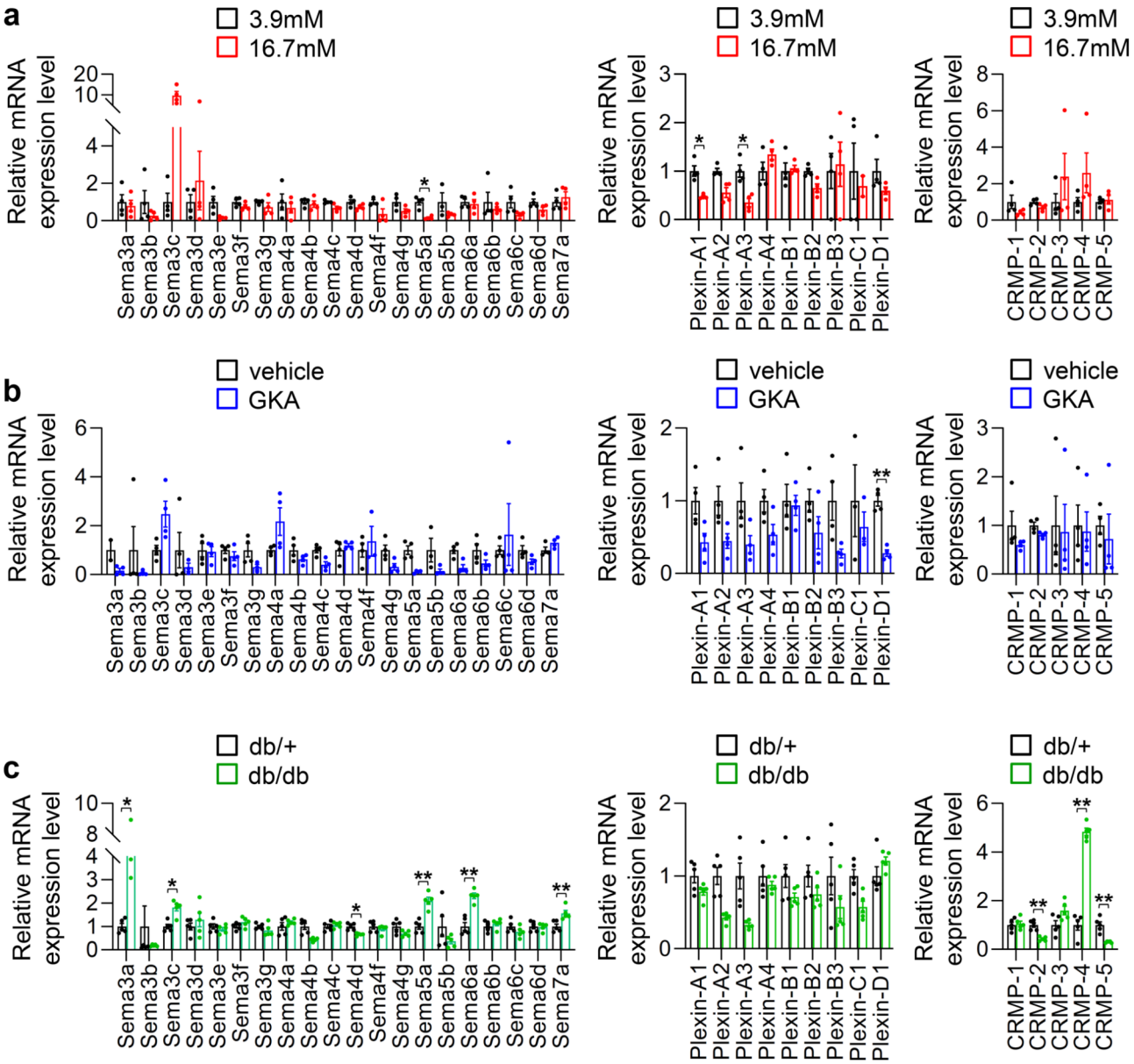

Fig. 4. Mouse pancreatic islet semaphorin, plexin, and CRMP levels under diabetic conditions. **a**-**c**: Semaphorin, plexin, and CRMP mRNA expression levels in isolated mouse islets. **a**: Islets were isolated from 8- to 10-week-old C57BL/6J mice and incubated in the presence of 3.9 or 16.7 mmol/L glucose for 24 h. **b**: Islets were isolated from 8- to 10-week-old C57BL/6J mice and incubated with GKA or vehicle (DMSO) for 24 h in the presence of 3.9 mmol/L glucose. **c**: Islets were isolated from 15-week-old *db/db* and *db/+* mice that were cultured for 24 h in the presence of 5.6 mmol/L glucose. $^{*}P<0.05$, $^{**}P<0.01$ ($n=4$–5 per group; multiple t-testing). The relative values were presented with C57BL/6J mouse islets under 3.9mM glucose (**a**), C57BL/6J mouse islets treated with vehicle (**b**), and *db/+* mouse islets (**c**) as the controls.

in insulin secretion (Fig. 6e-h). β-cell mass, glucose-induced insulin secretion, and the expression levels of key insulin signaling molecules, including *IRS-2*, *Pdx-1*, *MafA*, and *MafB*, were comparable between *CRMP-2*$^{-/-}$ and wild-type mice islets (Supplementary Fig. 3a-e). In contrast, the transcriptional factor *NeuroD1* expression was downregulated in *CRMP-2*$^{-/-}$ islets (Supplementary Fig. 3e). The degree of steatosis and fibrosis according to liver histology and the gene expression of *G6pc* and *Pck-1* were not altered in NC- or HF-fed *CRMP-2*$^{-/-}$ mice (Supplementary Fig. 3f-i).

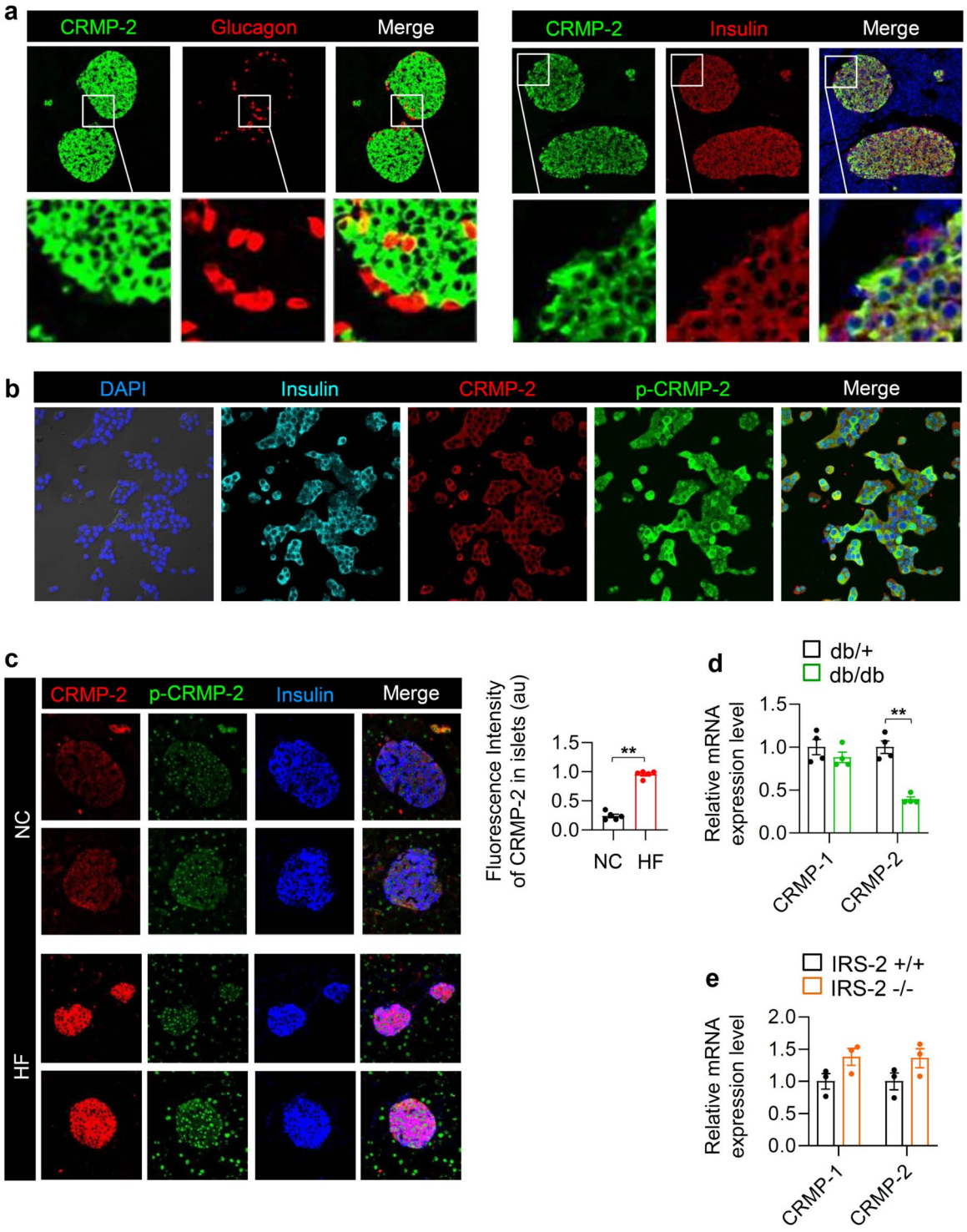

Discussion

In this study, we determined the distinct expression patterns of semaphorin/plexin/CRMP families in the endocrine pancreas, which were altered by glucose/glucokinase activation, and in *db/db* islets and demonstrated that *CRMP-2* knockout mice exhibited impaired glucose tolerance after HF feeding.

We demonstrated *Sema3c* expression in mouse pancreatic islets is precisely regulated by glucose signaling. High glucose stimulation increases IRS-2 expression in β-cells through the Ca^{2+}/calcineurin/NFAT pathway[25]. Consistent with this, we confirmed that glucokinase activation, which mimics hyperglycemia, upregulated the expression of *IRS-2*. This effect was attenuated by nifedipine, a calcium channel blocker, and FK506, a calcineurin inhibitor, in β-cells. Similarly, high glucose and glucokinase activation enhanced *Sema3c* in islets; however, this upregulation was only slightly observed in *IRS-2* knockout islets. Notably, unlike IRS-2, *Sema3c* upregulation by GKA was not inhibited by nifedipine or FK506, suggesting that glucokinase-induced *Sema3c* expression involves

◀**Fig. 5**. CRMP-2 was expressed in pancreatic β-cells. **a**: Pancreatic tissue sections from 8-12-week-old C57BL/6J mice were subjected to immunostaining. (Left) CRMP-2 was stained green, and glucagon was stained red. (Right) CRMP-2 was stained green, insulin was stained red, and nuclei were stained blue (DAPI). **b**: MIN6 cells were immunostained for nuclei (blue), insulin (light blue), CRMP-2 (red), and p-CRMP-2 (green). **c**:(Left) Pancreatic sections from C57BL/6J mice were immunostained with antibodies against CRMP-2 (red), p-CRMP-2 (green), and insulin (blue). (Upper) Normal chow (NC)-fed group at 8–12 weeks of age. (Lower) High-fat diet (HF)-fed group aged more than 20 weeks beginning at 8 weeks. (Right) Fluorescence intensity of CRMP-2 from ROI analysis of islets ($n = 5$; Student's t-test). **d**: The mRNA expression of *CRMP-1* and *CRMP-2* in islets from 12-week-old *db/db* and *db/+* mice cultured for 24 h in the presence of 5.6 mmol/L glucose ($n = 3$–4; Student's t-test). **e**: The mRNA expression of *CRMP-1* and *CRMP-2* in islets from 12-week-old *IRS-2* knockout and wild-type mice cultured for 24 h in the presence of 5.6 mmol/L glucose ($n = 3$–4; Student's t-test). The results are expressed as the mean ± SE. $^{**}P < 0.01$. The relative values were presented with *db/+* mouse islets (**d**), and *IRS-2*$^{+/+}$ mouse islets (**e**) as the controls.

both an IRS-2-dependent pathway and a separate pathway independent of Ca^{2+}/calcineurin-IRS-2 signaling. This is further supported by our finding that diazoxide, a K^+ ATP channel opener, did not affect GKA-induced *Sema3c* expression. In addition, IRS-2 may play a role in the upregulation of *Sema3c* observed in the islets of HF-fed mice, in which insulin signaling is known to be enhanced.

ER stress in islets induces β-cell apoptosis[29], which contributes to the onset of diabetes[30]. Short-term treatment with GKA suppressed the expression of ER stress-related genes and consequently protected β-cells from apoptosis in an IRS-2-independent manner[22]. Here, we showed that thapsigargin-induced ER stress enhanced the expression of *Sema3c*, and this effect was further amplified by high glucose stimulation, but not by GKA in islets. This suggests that the upregulation of *Sema3c* by GKA may be attributed to its inhibitory effect on ER stress in islets. Due to its involvement in glucose metabolism-related pathways, Sema3c may influence insulin secretion, β-cell proliferation, and apoptosis. Further study is needed to elucidate the precise effects and mechanisms of Sema3c action in islets.

To the best of our knowledge, this is the first report demonstrating the involvement of CRMPs in glucose metabolism. We detected the expression of CRMP-2 in primary mouse islets and MIN6 cells and found enhanced expression and phosphorylation of CRMP-2 in islets from HF-fed mice. CRMP-2 is an intracellular messenger of Sema3A[17] and Sema3B[31] signaling, and its phosphorylation mediates semaphorin signaling[32].

The involvement of CRMP-2 in Sema3C signaling remains unclear. Sema3C is co-expressed with Sema3A in the cortical midline and exerts its effects through a PLXNA1 and NRP1/2 heterodimer, playing a crucial role in regulating midline crossing during neuronal development[33,34]. Post-crossing repulsion has also been suggested to be mediated by Sema3A[34]. These findings imply a potential link between CRMP-2 function in glucose metabolism and Sema3C signaling within pancreatic islets. Our observation suggested that CRMP-2-mediated semaphorin signaling might be facilitated in pancreatic β-cells under HF feeding conditions. While the mild glucose intolerance in NC-fed *CRMP-1*$^{-/-}$ mice was alleviated by HF feeding, *CRMP-2*$^{-/-}$ mice showed impaired glucose tolerance in the HF-fed group but not in the NC-fed group. These results suggested that CRMP-2 acted under insulin resistance conditions, such as HF feeding. This is further supported by our observation in *db/db* mice, where *CRMP-2* gene expression in islets was significantly reduced compared to that in *db/+* mice, while *CRMP-1* mRNA expression remained unchanged.

CRMP-2$^{-/-}$ mice exhibited comparable insulin sensitivity and histology of insulin-sensitive organs including the liver. In HF-fed *CRMP-2*$^{-/-}$ mice, a slight reduction in β-cell mass or function was observed though it did not reach statistical significance. Gene expression levels of *IRS-2* and *Pdx-1* in *CRMP-2*$^{-/-}$ islets remained unchanged, suggesting that CRMP-2 has a minimal effect on insulin signaling. CRMP-2 modulates Ca^{2+} influx through presynaptic voltage-gated calcium channels during neurotransmitter release in neurons[35]. Therefore, CRMP deficiency might also cause calcium channel dysfunction, potentially impairing insulin secretion in β-cells.

In addition, considering that CRMP-2 is highly expressed in the nervous system and plays multiple roles in neuronal development, it is important to consider the potential involvement of neuronal signaling dysfunction in glucose intolerance. Pancreatic islets are extensively innervated by both parasympathetic and sympathetic nerves, which regulate insulin secretion and β-cell proliferation[36,37]. In *CRMP-2*$^{-/-}$ islets, the expression of *NeuroD1*, a transcriptional factor for maintaining β-cell maturation and a regulator of neuronal differentiation, was reduced. Furthermore, our comprehensive gene expression analysis of GKA-treated mouse islets revealed that glucose/glucokinase stimulation alters the expression of molecules associated with nervous system in islets, thereby influencing glucose metabolism. CRMPs are reportedly associated with neuropsychiatric disorders, especially schizophrenia[38,39]. It is well known that type 2 diabetes is significantly more prevalent in individuals with schizophrenia, with antipsychotic-naïve patients experiencing at least twice the risk of type 2 diabetes compared with healthy controls[40]. Our findings on the involvement of CRMPs in glucose metabolism may provide insight into the molecular basis underlying the comorbidity between type 2 diabetes and schizophrenia.

In summary, we revealed that the expression of semaphorins, plexins, and CRMPs was regulated in mouse islets by glucose/GKA stimulation or under diabetic conditions. We also demonstrated that *CRMP-2*$^{-/-}$ mice exhibited impaired glucose tolerance under HF conditions. Thus, the semaphorin/plexin/CRMP families in the endocrine pancreas might be involved in glucose metabolism through glucose/glucokinase signaling.

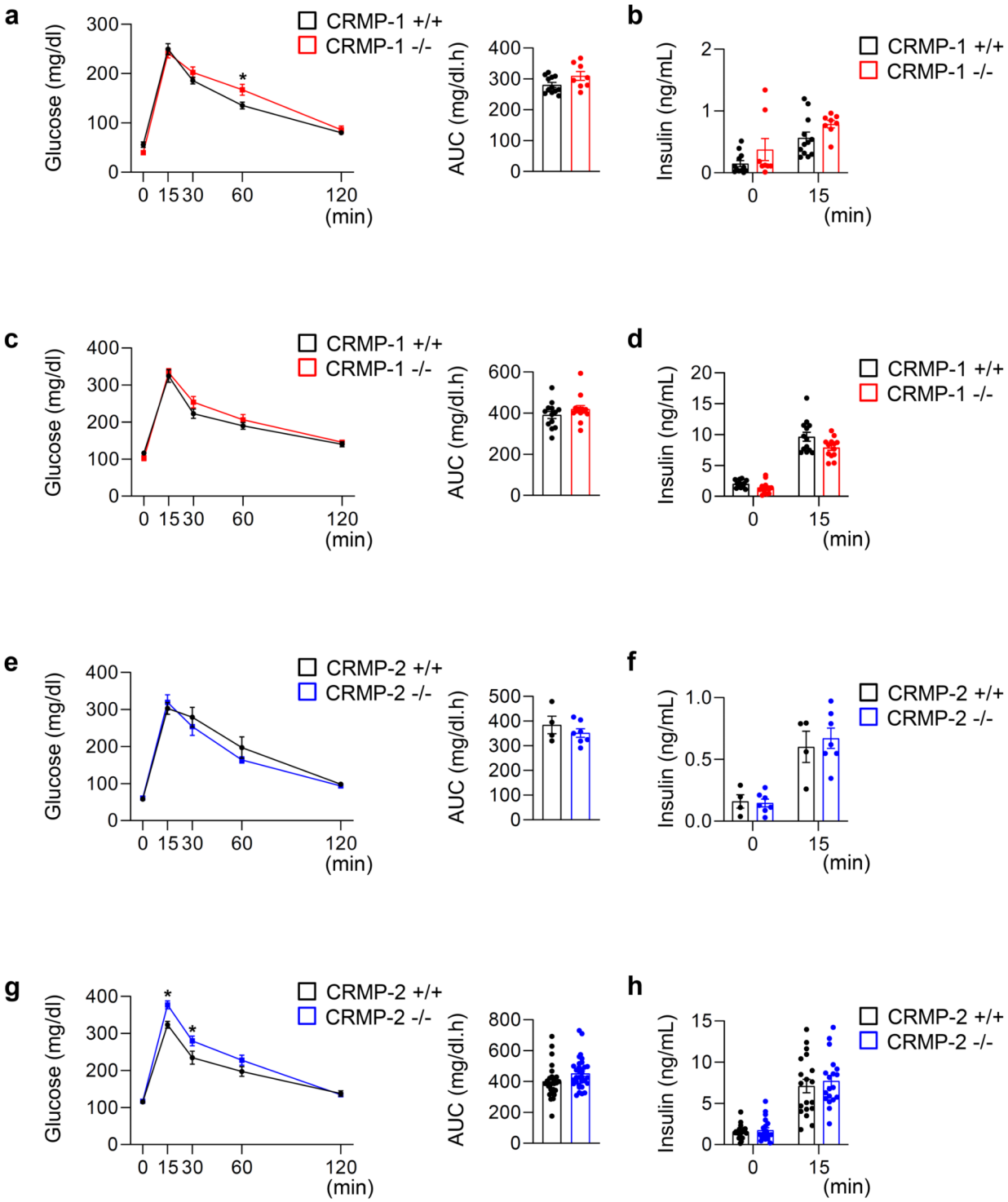

Fig. 6. GTTs and serum insulin levels of *CRMP-1*- and *CRMP-2*- knockout mice. **a**-**b**: The blood glucose levels and area under the curve (AUC) (**a**) and serum insulin levels (**b**) of *CRMP-1*$^{+/+}$ and *CRMP-1*$^{-/-}$ mice fed an NC were measured at the indicated times during the GTT. **c**-**d**: The blood glucose levels and AUCs (**c**) and serum insulin levels (**d**) of *CRMP-1*$^{+/+}$ and *CRMP-1*$^{-/-}$ mice fed an HF were measured at the indicated times during the GTT. **e**-**f**: The blood glucose levels and AUCs (**e**) and serum insulin levels (**f**) of *CRMP-2*$^{+/+}$ and *CRMP-2*$^{-/-}$ mice fed an NC were measured at the indicated times during the GTT. **g**-**h**: The blood glucose levels and AUCs (**g**) and serum insulin levels (**h**) of *CRMP-2*$^{+/+}$ and *CRMP-2*$^{-/-}$ mice fed HFs were measured at the indicated times during the GTT. The mice were fed an NC at 8–12 weeks of age or an HF for more than 20 weeks beginning at 8 weeks of age. The results are expressed as the mean ± SE. *$P < 0.05$ ($n = 8$–20 per group; Student's t-test).

Materials and methods

Animals and animal care

C57BL/6J mice were obtained from CLEA Japan (Tokyo, Japan). Both *CRMP-1*$^{-/-}$ mice and *CRMP-2*$^{-/-}$ mice on a C57BL/6J background were generated as described previously[41,42]. BKS. Cg-Dock7$^{m+/+}$Lepr^{db}/J (*db/db*) and their controls (*db/+*) were obtained from Charles River Japan (Yokohama, Japan). *IRS-2*$^{-/-}$ mice (CBA and C57BL/6J hybrid background) were generated as described elsewhere[23]. These mice were fed normal chow (MF, Oriental Yeast, Tokyo, Japan) or a high-fat diet (High Fat Diet 32, CLEA Japan) for 20 weeks beginning at 8 weeks. All the experiments were conducted on male littermates. The animal housing rooms were maintained at a constant room temperature (25 °C) and on a 12-hour light (7:00 AM) and 12-hour dark (7:00 PM) cycle. Mice were euthanized in a carbon dioxide chamber.

Animal study approval

This study was conducted with the approval of the Animal Care Committee of Yokohama City University (approval no. F-A-13-043). All the animal procedures and experimental protocols were performed in accordance with the institutional animal care guidelines and the guidelines of the Animal Care Committee of Yokohama City University. The study was conducted in accordance with the ARRIVE guidelines.

In vivo physiological studies

The plasma glucose levels and blood insulin levels were determined using a Glutest Neo Super (Sanwa Kagaku Kenkyusho, Nagoya, Japan) and an insulin kit (Morinaga, Yokohama, Japan; catalog no. M1102). All the mice were denied access to food overnight before the oral glucose tolerance test (GTT) and then were orally loaded with glucose (1.5 mg/g body weight). The insulin tolerance test (ITT) was performed by ip injection of human insulin at 1.5 mU/g body weight without fasting (normal chow-fed group) and 2 mU/g body weight after 2 h of fasting (high-fat diet-fed group).

Islet isolation and culture

Islets were isolated from the mice as described elsewhere[43]. Isolated islets were cultured overnight in RPMI 1640 medium (Wako Pure Chemical Industries, Osaka, Japan) containing 5.6 mmol/L glucose supplemented with 10% fetal calf serum, 100 units/mL penicillin, and 100 µg/mL streptomycin. Islets were treated with 1 µmol/L thapsigargin (Nacalai Tesque, Tokyo, Japan), 50 µmol/L nifedipine (Sigma-Aldrich, St. Louis, MO), 10 µmol/L FK506 (Sigma-Aldrich), 30 µmol/L GKA Cpd A (Calbiochem, Darmstadt, Germany)[44], 10 mmol/L D-mannoheptulose (Toronto Research Chemicals, Toronto, Canada), or 200 µmol/L diazoxide (Wako Pure Chemical Industries). All the reagents were added concomitantly to the medium in each experiment.

Glucose-stimulated insulin secretion in isolated islets

Ten islets isolated from high-fat diet-fed *CRMP-2*$^{+/+}$ mice and *CRMP-2*$^{-/-}$ mice were incubated at 37 °C for 1.5 h in Krebs-Ringer bicarbonate buffer containing 2.8 or 22.2 mmol/L glucose. To measure the insulin content, the islets were extracted with acid ethanol. The insulin concentration of the assay buffer and the insulin content were measured using an insulin ELISA kit (Morinaga).

Cell culture

MIN6 cells were a kind gift from Dr. Junichi Miyazaki (University of Osaka, Osaka, Japan)[45]. MIN6 cells were cultured in DMEM containing 11.1 mmol/L glucose supplemented with 10% fetal calf serum, 100 units/mL penicillin, 100 µg/mL streptomycin, and 0.002% 2-mercaptoethanol.

Histological analysis

Formalin-fixed, paraffin-embedded pancreas sections and 4% paraformaldehyde-fixed MIN6 cells on cover slides were immunostained with antibodies against insulin (Santa Cruz, CA), glucagon (Abcam, Cambridge, UK), CRMP-2 or p-CRMP-2 (as described elsewhere[46]). Alexa Fluor 488-, 555-, and 647-conjugated secondary antibodies (Invitrogen, Carlsbad, CA) were used for fluorescence microscopic analysis. Images were acquired using a FluoView FV1000-D confocal laser scanning microscope (Olympus, Southborough, MA). The fluorescence intensity of CRMP-2 was calculated in 5 randomly selected areas per islet using ImageJ software (http://imagej.nih.gov/ij, using version 1.53k), and the normalized intensity of insulin is shown in the graph. Biotinylated secondary antibodies, a VECTASTAIN Elite ABC Kit, and a DAB Substrate Kit (Vector Laboratories, Burlingame, CA) were used to examine the sections using bright-field microscopy to determine the β-cell mass. Images were acquired using a BZ-9000 microscope (Keyence, Osaka, Japan). The percent area of the pancreatic tissue occupied by the β-cells was calculated using the software provided with BIOREVO BZ-9000 (Keyence), as described elsewhere[43]. Formalin-fixed, paraffin-embedded liver sections were stained with Masson Goldner.

Real-time PCR

Total RNA from the liver, skeletal muscle, and pancreatic islets was isolated using a QIA shredder and an RNeasy kit (QIAGEN, Hilden, Germany). Total RNA from the cerebral cortex, olfactory bulb, and epididymal fat was isolated using an Isogen reagent (Nippon Gene, Toyama, Japan) and an RNeasy kit (QIAGEN). cDNA was prepared using High-Capacity cDNA reverse transcription kits (Applied Biosystems, Foster City, CA, USA) and subjected to quantitative PCR (7900 real-time PCR system; Applied Biosystems) using THUNDERBIRD qPCR Master Mix (Toyobo, Osaka, Japan) for Taqman assays (Fig. 2a-j and 5d-e, Supplementary Fig. 3e, 3g-i) or THUNDERBIRD SYBR qPCR Master Mix (Toyobo) for SYBR Green assays (Fig. 3a-c and 4a-c, Supplementary Fig. 3e). The relative values were presented with C57BL/6J mouse islets treated with vehicle after 2 h incubation (Fig. 2a), C57BL/6J mouse islets under 2.8mM glucose (Fig. 2b and i), *IRS-2*$^{+/+}$ mouse islets treated with vehicle

(Fig. 2c), *db*/+ mouse islets treated with vehicle (Fig. 2d), normal chow (NC)-fed mouse islets treated with vehicle (Fig. 2e), C57BL/6J mouse islets treated with vehicle (Fig. 2f-h and j, and 4b), C57BL/6J mouse islets treated with vehicle under 2.8mM glucose (Fig. 2i), cerebral cortex (Fig. 3a-c), C57BL/6J mouse islets under 3.9mM glucose (Fig. 4a), *db*/+ mouse islets (Figs. 4c and 5d), and *IRS-2*$^{+/+}$ mouse islets (Fig. 5e) as the controls. Each quantitative reaction was performed in duplicate. The data were normalized to the β-actin level. For the Taqman assay, primers were purchased from Applied Biosystems. The SYBR Green primers used are listed in Supplementary Table 2.

Single-cell RNA sequencing

Isolated mouse pancreatic islets from normal chow diet-fed and 8-week high fat-diet fed mice for single-cell RNA sequencing using a method described elsewhere[47]. The single-cell RNA-seq data we used in this study are available from Gene Expression Omnibus (GEO) with the accession numbers GSE203376[26].

Statistical analysis

All the data are reported as the means ± SEs and were analyzed using Student's *t* test, multiple t-testing, or ANOVA in the GraphPad Prism 8 (https://www.graphpad.com/scientific-software/prism/, using version 8.0.2; GraphPad). Differences were considered significant if the *P* value was < 0.05 (*) or < 0.01 (**).

Data availability

All the data analyzed during this study are included in this article and its Supplementary Information files.

Received: 25 May 2024; Accepted: 20 March 2025
Published online: 27 March 2025

References

1. Shirakawa, J. Signaling pathways that regulate adaptive β-cell proliferation for the treatment of diabetes. *J. Diabetes Invest.* **14**, 735–740. https://doi.org/10.1111/jdi.14002 (2023).
2. Shirakawa, J. & Terauchi, Y. Newer perspective on the coupling between glucose-mediated signaling and β-cell functionality. *Endocr. J.* **67**, 1–8. https://doi.org/10.1507/endocrj.EJ19-0335 (2020).
3. Shirakawa, J. Translational research on human pancreatic β-cell mass expansion for the treatment of diabetes. *Diabetol. Int.* **12**, 349–355. https://doi.org/10.1007/s13340-021-00531-4 (2021).
4. Yazdani, U. & Terman, J. R. The semaphorins. *Genome Biol.* **7**, 211. https://doi.org/10.1186/gb-2006-7-3-211 (2006).
5. Zhou, Y., Gunput, R. A. & Pasterkamp, R. J. Semaphorin signaling: Progress made and promises ahead. *Trends Biochem. Sci.* **33**, 161–170. https://doi.org/10.1016/j.tibs.2008.01.006 (2008).
6. Takamatsu, H. & Kumanogoh, A. Diverse roles for semaphorin-plexin signaling in the immune system. *Trends Immunol.* **33**, 127–135. https://doi.org/10.1016/j.it.2012.01.008 (2012).
7. Epstein, J. A., Aghajanian, H. & Singh, M. K. Semaphorin signaling in cardiovascular development. *Cell Metabol.* **21**, 163–173. https://doi.org/10.1016/j.cmet.2014.12.015 (2015).
8. Verlinden, L., Vanderschueren, D. & Verstuyf, A. Semaphorin signaling in bone. *Mol. Cell. Endocrinol.* **432**, 66–74. https://doi.org/10.1016/j.mce.2015.09.009 (2016).
9. Tamagnone, L. Emerging role of semaphorins as major regulatory signals and potential therapeutic targets in cancer. *Cancer Cell.* **22**, 145–152. https://doi.org/10.1016/j.ccr.2012.06.031 (2012).
10. Shimizu, I. et al. Semaphorin3E-induced inflammation contributes to insulin resistance in dietary obesity. *Cell Metabol.* **18**, 491–504. https://doi.org/10.1016/j.cmet.2013.09.001 (2013).
11. Aggarwal, P. K. et al. Semaphorin3a promotes advanced diabetic nephropathy. *Diabetes* **64**, 1743–1759. https://doi.org/10.2337/db14-0719 (2015).
12. Perälä, N., Sariola, H. & Immonen, T. More than nervous: The emerging roles of plexins. *Differ. Res. Biol. Divers.* **83**, 77–91. https://doi.org/10.1016/j.diff.2011.08.001 (2012).
13. Jongbloets, B. C. & Pasterkamp, R. J. Semaphorin signalling during development. *Dev. (Camb. Engl.)* **141**, 3292–3297. https://doi.org/10.1242/dev.105544 (2014).
14. Kong, Y. et al. Structural basis for Plexin activation and regulation. *Neuron* **91**, 548–560. https://doi.org/10.1016/j.neuron.2016.06.018 (2016).
15. Goshima, Y., Nakamura, F., Strittmatter, P. & Strittmatter, S. M. Collapsin-induced growth cone collapse mediated by an intracellular protein related to UNC-33. *Nature* **376**, 509–514. https://doi.org/10.1038/376509a0 (1995).
16. Minturn, J. E., Fryer, H. J., Geschwind, D. H. & Hockfield, S. TOAD-64, a gene expressed early in neuronal differentiation in the rat, is related to unc-33, a C. elegans gene involved in axon outgrowth. *J. Neurosci. Off. J. Soc. Neurosci.* **15**, 6757–6766 (1995).
17. Schmidt, E. F. & Strittmatter, S. M. The CRMP family of proteins and their role in Sema3A signaling. *Adv. Exp. Med. Biol.* **600**, 1–11. https://doi.org/10.1007/978-0-387-70956-7_1 (2007).
18. Quach, T. T. et al. Involvement of collapsin response mediator proteins in the neurite extension induced by neurotrophins in dorsal root ganglion neurons. *Mol. Cell. Neurosci.* **25**, 433–443. https://doi.org/10.1016/j.mcn.2003.11.006 (2004).
19. Yoshimura, T. et al. GSK-3beta regulates phosphorylation of CRMP-2 and neuronal Polarity. *Cell* **120**, 137–149. https://doi.org/10.1016/j.cell.2004.11.012 (2005).
20. Wakatsuki, S., Saitoh, F. & Araki, T. ZNRF1 promotes wallerian degeneration by degrading AKT to induce GSK3B-dependent CRMP2 phosphorylation. *Nat. Cell Biol.* **13**, 1415–1423. https://doi.org/10.1038/ncb2373 (2011).
21. Zhao, J. et al. PTEN inhibition prevents rat cortical neuron injury after hypoxia-ischemia. *Neuroscience* **238**, 242–251. https://doi.org/10.1016/j.neuroscience.2013.02.046 (2013).
22. Shirakawa, J. et al. Glucokinase activation ameliorates ER stress-induced apoptosis in pancreatic beta-cells. *Diabetes* **62**, 3448–3458. https://doi.org/10.2337/db13-0052 (2013).
23. Kubota, N. et al. Disruption of insulin receptor substrate 2 causes type 2 diabetes because of liver insulin resistance and lack of compensatory beta-cell hyperplasia. *Diabetes* **49**, 1880–1889 (2000).
24. Chen, H. et al. Evidence that the diabetes gene encodes the leptin receptor: Identification of a mutation in the leptin receptor gene in Db/db mice. *Cell* **84**, 491–495 (1996).
25. Demozay, D., Tsunekawa, S., Briaud, I., Shah, R. & Rhodes, C. J. Specific glucose-induced control of insulin receptor substrate-2 expression is mediated via Ca2+-dependent Calcineurin/NFAT signaling in primary pancreatic islet beta-cells. *Diabetes* **60**, 2892–2902. https://doi.org/10.2337/db11-0341 (2011).

26. Fu, Q. et al. Single-cell RNA sequencing combined with single-cell proteomics identifies the metabolic adaptation of islet cell subpopulations to high-fat diet in mice. *Diabetologia* **66**, 724–740. https://doi.org/10.1007/s00125-022-05849-5 (2023).
27. Nakatsuji, Y. et al. Elevation of Sema4A implicates Th cell skewing and the efficacy of IFN-β therapy in multiple sclerosis. *J. Immunol. (Baltimore Md. 1950)*. **188**, 4858–4865. https://doi.org/10.4049/jimmunol.1102023 (2012).
28. Wang, L. H. & Strittmatter, S. M. Brain CRMP forms heterotetramers similar to liver dihydropyrimidinase. *J. Neurochem.* **69**, 2261–2269 (1997).
29. Laybutt, D. R. et al. Endoplasmic reticulum stress contributes to beta cell apoptosis in type 2 diabetes. *Diabetologia* **50**, 752–763. https://doi.org/10.1007/s00125-006-0590-z (2007).
30. Butler, A. E. et al. Beta-cell deficit and increased beta-cell apoptosis in humans with type 2 diabetes. *Diabetes* **52**, 102–110 (2003).
31. Arbeille, E. et al. Cerebrospinal fluid-derived Semaphorin3B orients neuroepithelial cell divisions in the apicobasal axis. *Nat. Commun.* **6**, 6366. https://doi.org/10.1038/ncomms7366 (2015).
32. Uchida, Y. et al. Semaphorin3A signalling is mediated via sequential Cdk5 and GSK3beta phosphorylation of CRMP2: Implication of common phosphorylating mechanism underlying axon guidance and Alzheimer's disease. *Genes Cells Devot. Mol. Cell. Mech.* **10**, 165–179. https://doi.org/10.1111/j.1365-2443.2005.00827.x (2005).
33. Piper, M. et al. Neuropilin 1-Sema signaling regulates crossing of cingulate pioneering axons during development of the corpus callosum. *Cereb. Cortex (New York N Y 1991)*. **19** (Suppl 1), i11–21. https://doi.org/10.1093/cercor/bhp027 (2009).
34. Limoni, G. & Niquille, M. Semaphorins and plexins in central nervous system patterning: The key to it all? *Curr. Opin. Neurobiol.* **66**, 224–232. https://doi.org/10.1016/j.conb.2020.12.014 (2021).
35. Wang, Y., Brittain, J. M., Wilson, S. M. & Khanna, R. Emerging roles of collapsin response mediator proteins (CRMPs) as regulators of voltage-gated calcium channels and synaptic transmission. *Commun. Integr. Biol.* **3**, 172–175. https://doi.org/10.4161/cib.3.2.10620 (2010).
36. Ahrén, B. Autonomic regulation of islet hormone secretion–implications for health and disease. *Diabetologia* **43**, 393–410. https://doi.org/10.1007/s001250051322 (2000).
37. Kawana, Y. et al. Optogenetic stimulation of vagal nerves for enhanced glucose-stimulated insulin secretion and B cell proliferation. *Nat. Biomed. Eng.* https://doi.org/10.1038/s41551-023-01113-2 (2023).
38. Quach, T. T., Honnorat, J., Kolattukudy, P. E., Khanna, R. & Duchemin, A. M. CRMPs: Critical molecules for neurite morphogenesis and neuropsychiatric diseases. *Mol. Psychiatry*. **20**, 1037–1045. https://doi.org/10.1038/mp.2015.77 (2015).
39. Ramos, A. et al. Proteomic studies reveal disrupted in schizophrenia 1 as a player in both neurodevelopment and synaptic function. *Int. J. Mol. Sci.* **20** https://doi.org/10.3390/ijms20010119 (2018).
40. Stubbs, B., Vancampfort, D., De Hert, M. & Mitchell, A. J. The prevalence and predictors of type two diabetes mellitus in people with schizophrenia: A systematic review and comparative meta-analysis. *Acta Psychiatry. Scand.* **132**, 144–157. https://doi.org/10.1111/acps.12439 (2015).
41. Yamashita, N. et al. Mice lacking collapsin response mediator protein 1 manifest hyperactivity, impaired learning and memory, and impaired prepulse Inhibition. *Front. Behav. Neurosci.* **7**, 216. https://doi.org/10.3389/fnbeh.2013.00216 (2013).
42. Nakamura, H. et al. Comprehensive behavioral study and proteomic analyses of CRMP2-deficient mice. *Genes Cells Devoted Mol. Cell. Mech.* **21**, 1059–1079. https://doi.org/10.1111/gtc.12403 (2016).
43. Shirakawa, J. et al. Protective effects of dipeptidyl peptidase-4 (DPP-4) inhibitor against increased beta cell apoptosis induced by dietary sucrose and Linoleic acid in mice with diabetes. *J. Biol. Chem.* **286**, 25467–25476. https://doi.org/10.1074/jbc.M110.217216 (2011).
44. Futamura, M. et al. An allosteric activator of glucokinase impairs the interaction of glucokinase and glucokinase regulatory protein and regulates glucose metabolism. *J. Biol. Chem.* **281**, 37668–37674. https://doi.org/10.1074/jbc.M605186200 (2006).
45. Miyazaki, J. et al. Establishment of a pancreatic beta cell line that retains glucose-inducible insulin secretion: special reference to expression of glucose transporter isoforms. *Endocrinology* **127**, 126–132. https://doi.org/10.1210/endo-127-1-126 (1990).
46. Uchida, Y. et al. Semaphorin3A signaling mediated by Fyn-dependent tyrosine phosphorylation of collapsin response mediator protein 2 at tyrosine 32. *J. Biol. Chem.* **284**, 27393–27401. https://doi.org/10.1074/jbc.M109.000240 (2009).
47. Okuyama, T. et al. The matricellular protein Fibulin-5 regulates β-cell proliferation in an autocrine/paracrine manner. *iScience* **28**, 111856. https://doi.org/10.1210/endocr/bqad095 (2025).

Acknowledgements

We thank Dr. Takashi Kadowaki and Dr. Naoto Kubota (Department of Diabetes and Metabolic Disease, Graduate School of Medicine, University of Tokyo, Tokyo, Japan) for kindly gifting the *IRS-2*$^{-/-}$ mice. We thank Mitsuyo Kaji (Yokohama City University) for technical assistance.

Author contributions

M.K. conducted the research and contributed to the discussion and writing of the manuscript. R.T., T.T., E.O.Y. and K.N. conducted the research. T.T., E.O.Y., R.I., N.Y., T.O., K.M., E.I., S.I., Y.T. and Y.G. contributed to the discussion and edited the manuscript. J.S. contributed to the design and conception of the study and the writing of the manuscript, contributed to the discussion, and reviewed and edited the manuscript. All the authors reviewed the manuscript and approved the final version.

Declarations

Competing interests

The authors declare no competing interests.

Additional information

Supplementary Information The online version contains supplementary material available at https://doi.org/10.1038/s41598-025-95300-7.

Correspondence and requests for materials should be addressed to J.S.

Reprints and permissions information is available at www.nature.com/reprints.

Publisher's note Springer Nature remains neutral with regard to jurisdictional claims in published maps and institutional affiliations.

Open Access This article is licensed under a Creative Commons Attribution-NonCommercial-NoDerivatives 4.0 International License, which permits any non-commercial use, sharing, distribution and reproduction in any medium or format, as long as you give appropriate credit to the original author(s) and the source, provide a link to the Creative Commons licence, and indicate if you modified the licensed material. You do not have permission under this licence to share adapted material derived from this article or parts of it. The images or other third party material in this article are included in the article's Creative Commons licence, unless indicated otherwise in a credit line to the material. If material is not included in the article's Creative Commons licence and your intended use is not permitted by statutory regulation or exceeds the permitted use, you will need to obtain permission directly from the copyright holder. To view a copy of this licence, visit http://creativecommons.org/licenses/by-nc-nd/4.0/.

© The Author(s) 2025